Journal of Biomedical Optics 9(1), 213–220 (January/February 2004)

Balanced detection for low-noise precision polarimetric measurements of optically active, multiply scattering tissue phantoms

D. Côté
Ontario Cancer Institute
University Health Network
and
University of Toronto
Department of Medical Biophysics
Ontario, Canada M5G 2M9
E-mail: dcote@uhnres.utoronto.ca

I. A. Vitkin
Ontario Cancer Institute
University Health Network
and
University of Toronto
Department of Medical Biophysics
Radiation Oncology
Ontario, Canada M5G 2M9

Abstract. The use and advantages of balanced detection for making low-noise polarimetric measurements in turbid materials are demonstrated. The technique reduces the intensity noise originating from the laser and, in addition, makes possible a direct measurement of a component of the Stokes vector. When phase-locked detection is used with either amplitude or polarization modulation for polarimetric measurements in turbid media, one can obtain elements of the scattering matrix of very small magnitude. This methodology is used to measure optical activity and surviving linear polarization fractions in clear and turbid media containing glucose at physiologically relevant concentrations. The results are in agreement with Monte Carlo simulations of polarized light propagation in turbid media. [DOI: 10.1117/1.1629683]

Keywords: glucose; optical activity; polarimetry; multiple scattering; turbid; Stokes parameters.

Paper 03064 received May 15, 2003; revised manuscript received Jul. 25, 2003; accepted for publication Jul. 28, 2003.

1 Introduction

In recent years, there has been an increased interest in using nonharmful light for studying and diagnosing human pathologies because of the noninvasive nature of the light–tissue interaction. One medical condition of particular clinical importance is diabetes, with its associated need for monitoring blood glucose. In order to overcome the discomfort to the patient caused by current commercial devices that require small blood samples, noninvasive glucose monitoring techniques have been investigated by several research groups.[1] Polarimetric measurements of optical activity that is due to glucose in the aqueous humor of the eye, for instance, have shown great promise recently since the eye is the only transparent tissue in the body. However, birefringence of the cornea and multiple reflections in its layered geometry make measurements and their interpretation difficult.[2] For this and other reasons, measurements performed at other sites on the body should be investigated, including areas that are optically thick.

However, while the propagation of light in a transparent medium such as the eye is well described by Maxwell's equation, the propagation of light in tissue is more complicated and is better modeled as a combination of scattering and bulk dielectric propagation. Because of the high number of scattering events in tissues, it is natural at first to disregard the polarization of light in models since the scatterers randomize—and eventually completely scramble—the polarization of light.[3] Light propagation in tissue is commonly modeled within the framework of light transport theory or diffusion theory, assuming that the particle nature of light is sufficient to describe all the relevant properties of the measurements.[3] Monte Carlo calculations, together with some aspects of Mie theory, have become standard for predicting and modeling experiments.[4]

Recently, however, the polarization of light has been used to extract quantitative information from the optically thick tissues with which it interacts. Indeed, although the degree of polarization is significantly lowered after propagating through thick turbid media, often it is not completely destroyed.[5] Polarization is well suited for measuring birefringence and optical activity, which affect, respectively, the ellipticity and the orientation of the polarization of the incident beam. For instance, it has been used in tissue birefringence measurement,[6] polarization-sensitive optical coherence tomography (OCT) measurements,[7,8] and imaging of polarization-sensitive skin pathology[9] to yield more information about the tissue than is provided by intensity data alone. In the case of noninvasive glucose monitoring, it has been shown that the presence of glucose can be detected in turbid media via index-matching effects that lower the tissue scattering coefficient.[10,11] However, it is difficult to measure absolute concentrations of the glucose when relying on a change in the scattering coefficient since other factors can affect the scattering (tissue inhomogeneity, for example). Other methods based on optical activity[12] effects have also been used to quantify the presence of glucose in turbid media, and offer a more direct method for glucose quantification since the optical rotation is linear with the glucose concentration. However, the small physiological blood glucose concentration (typically 10 mM) yields a very small optical rotation, on the order of millidegrees through 1 cm of tissue. Since many polarimetric measurements rely on taking the difference of two intensity readings at two orthogonal polarizations, measurements of small polarimetric signals in the presence of a large depolarized background are difficult to perform, especially in the presence of significant low-frequency laser noise.

1083-3668/2004/$15.00 © 2004 SPIE

In the past, we have used a technique that relies on taking multiple measurements at different analyzer optic orientations and performing an analytical fitting procedure based on the expected dependence of the signal on the orientation to obtain precise values of the induced optical rotation and depolarizing parameters.[12,13] In this paper we demonstrate how to perform sensitive polarimetric measurements in highly scattering media ($\mu_s \approx 30\ \mathrm{cm}^{-1}$) without the need for multiple measurements or user adjustments. The key to the method is to perform two measurements simultaneously and electronically subtract them before doing lock-in detection, thereby canceling any common-mode noise at the receivers (e.g., laser intensity or any polarization-independent noise). The laser used in the experiments is not stabilized in intensity, but the methodology developed here is general and would cancel any remaining intensity noise in a setup that makes use of an intensity-stabilized laser (these lasers typically have a 0.01% noise root mean square in intensity).

There are experimental techniques[14,15] that allow the complete characterization of the scattering matrix of a sample without any moving parts. The technique presented here, on the other hand, does not attempt to fully characterize the scattering matrix. Instead, it concentrates on a few elements that are important for characterizing optical activity. The strength of this methodology lies in its ability to measure small elements of the scattering matrix. To compare our measurements with predictions, we use a Monte Carlo model that includes polarization effects based on publications by other groups.[16–18]

This paper proceeds as follows. First, the formalism used to model the experiments is reviewed, together with the definitions of the relevant parameters. This is used to introduce the rationale for the balanced detection method. The experimental setup for the measurements of glucose concentrations at physiologically relevant levels in turbid media is described, and the methodology for measurements and analysis is presented. Finally, the effects of turbidity and glucose on light polarization are measured and shown to be in agreement with published experimental values and polarization-sensitive Monte Carlo predictions.

2 Formalism

It is common to describe polarized light using Stokes parameters. The state of polarization of the light, with respect to a chosen set of orthonormal axes $\hat{e}_\parallel$ and $\hat{e}_\perp$, is given by a Stokes vector **S** of the form:

$$\mathbf{S}=\begin{bmatrix} I \\ Q \\ U \\ V \end{bmatrix}, \tag{1}$$

where the same notation and definitions as in Bohren and Huffman[19] are used (see Fig. 1). We have:

$$I \equiv E_\parallel E_\parallel^* + E_\perp E_\perp^*, \tag{2}$$

$$Q \equiv E_\parallel E_\parallel^* - E_\perp E_\perp^*, \tag{3}$$

$$U \equiv E_\parallel E_\perp^* + E_\parallel^* E_\perp, \tag{4}$$

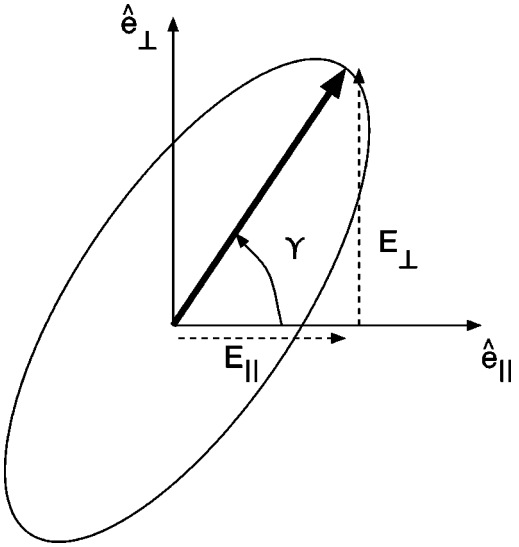

Fig. 1 The complex electric field is decomposed into two perpendicular components $E_\parallel$ and $E_\perp$. The reference axis $\hat{e}_\parallel$ ($\hat{e}_\perp$) refers to a direction parallel (perpendicular) to the scattering plane, which in the situation of interest here is horizontal (vertical) in the laboratory frame. The ellipsometric parameter γ (the orientation of the major axis of the polarization ellipse with respect to $\hat{e}_\parallel$) is shown in the figure.

$$V \equiv i(E_\parallel E_\perp^* - E_\parallel^* E_\perp), \tag{5}$$

with $E_\parallel$ and $E_\perp$ the complex electric field components (with their complex conjugate $E_\parallel^*$ and $E_\perp^*$, and $i \equiv \sqrt{-1}$). I represents the intensity of the beam, Q and U represent the linear polarization (respectively in the frame of reference made of $\hat{e}_\parallel$ and $\hat{e}_\perp$, and in another frame rotated by 45 deg with respect to the former), and V represents the circular polarization. The degree of linear polarization (DOP_L) is defined as

$$DOP_L = \frac{(Q^2+U^2)^{1/2}}{I}, \tag{6}$$

where DOP_L ranges from 1 (for fully linearly polarized light) to 0 (for fully unpolarized light or fully circularly polarized light), with values between 0 and 1 for partially linearly polarized light. For example, light completely linearly polarized, making an angle of 0 deg with $\hat{e}_\parallel$ has a Stokes vector:

$$\mathbf{S}_0=\begin{bmatrix} 1 \\ 1 \\ 0 \\ 0 \end{bmatrix}. \tag{7}$$

The Stokes vector provides all the necessary information related to the polarization state of the light beam. Of interest here is the angle γ of the major axis of the polarization ellipse with respect to $\hat{e}_\parallel$, which can be obtained from the Stokes parameters with

$$\tan 2\gamma = \frac{U}{Q}. \tag{8}$$

The change in the orientation γ of the polarization ellipse of a beam is α, the rotation of the plane of polarization, a quantity of interest that is induced by the optical activity of glucose in subsequent experiments.

To streamline the mathematics, it is convenient to define ''detector'' operators. When one applies the detector operator to a Stokes vector **S**, the scalar value of that particular Stokes parameter is obtained. Mathematically, detector operators for the first three Stokes parameters are defined as

$$\mathbf{I}^{\dagger}=[1\ \ 0\ \ 0\ \ 0], \tag{9}$$

$$\mathbf{Q}^{\dagger}=[0\ \ 1\ \ 0\ \ 0], \tag{10}$$

$$\mathbf{U}^{\dagger}=[0\ \ 0\ \ 1\ \ 0]. \tag{11}$$

The intensity detection operator $\mathbf{I}^{\dagger}$ corresponds to a measurement of the intensity of a beam with a photodetector. It will be shown later that it is possible to use two intensity detectors in conjunction with a polarizing beamsplitter to experimentally implement the detection operator $\mathbf{Q}^{\dagger}$.

Upon propagation through optical elements or scattering with an object, the Stokes vector of a beam is transformed. This can be described with the multiplication of the Stokes vector by Mueller matrices representing the interactions. Mueller matrices for the propagation through standard optical elements [polarizer $\mathbf{P}(\theta)$, wave plate, etc.] are known and will not be repeated here.[19] When a beam encounters a scatterer, the incident field will be redistributed in all directions, depending on the properties of the scatterer, the surrounding medium, and the illumination wavelength. A scattering direction is completely determined with two angles. The scattering angle θ is the angle between the incident propagation direction $\hat{z}$ and the new direction of propagation of the field $\hat{z}'$. The plane spanned by $\hat{z}$ and $\hat{z}'$ is called the scattering plane, and the azimuthal angle ϕ is the orientation of $\hat{e}_{\parallel}$ with respect to that scattering plane. In general, one represents a multiply scattering medium by an arbitrary matrix $\boldsymbol{\mathcal{M}}$:

$$\boldsymbol{\mathcal{M}}=\begin{bmatrix} m_{11} & m_{12} & m_{13} & m_{14} \\ m_{21} & m_{22} & m_{23} & m_{24} \\ m_{31} & m_{32} & m_{33} & m_{34} \\ m_{41} & m_{42} & m_{43} & m_{44} \end{bmatrix}. \tag{12}$$

Using Mie theory, one can calculate the Mueller matrix elements of simple single scatterers. In general, the matrix elements depend strongly on the scattering angle θ and scattering is therefore anisotropic. A single spherical scatterer, for instance, has a scattering matrix of the form:

$$\begin{bmatrix} a(\theta) & b(\theta) & 0 & 0 \\ b(\theta) & a(\theta) & 0 & 0 \\ 0 & 0 & d(\theta) & e(\theta) \\ 0 & 0 & -e(\theta) & d(\theta) \end{bmatrix}, \tag{13}$$

where the parameters $a(\theta), b(\theta), d(\theta)$, and $e(\theta)$ can be calculated with the help of Mie theory.[20] The directional dependence of scattering is characterized with an anisotropy parameter g, which is the average cosine of the scattering angle $\langle \cos\theta \rangle$. Biological tissues typically exhibit forward scattering, with $g > 0.9$. Although the Mueller matrix of a single scatterer can be deduced from Mie theory, that of a collection of scatterers, representing a multiply scattering medium, cannot in general be calculated analytically. Certain properties of the matrix can be deduced from symmetry arguments,[21] but Monte Carlo methods are most often used to simulate light propagation in an optically thick turbid medium. With polarization-sensitive implementation, Monte Carlo results yield numerical values for the Mueller matrix elements in Eq. (12), as is done in the present work.

In order to determine the optical activity of a turbid medium, we use two important ratios: m_{32}/m_{22} and m_{22}/m_{11}. The ratio m_{32}/m_{22} is a direct measurement of optical rotation α, which can be understood from the following argument. Using Eqs. (7) and (8), the orientation for a horizontally polarized beam with the incident Stokes vector $\mathbf{S}_0$ is

$$\gamma=\frac{1}{2}\tan^{-1}\left(\frac{\mathbf{U}^{\dagger}\mathbf{S}_0}{\mathbf{Q}^{\dagger}\mathbf{S}_0}\right)=0, \tag{14}$$

whereas upon interaction with a medium, the new orientation γ' is obtained by definition with:

$$\gamma'=\frac{1}{2}\tan^{-1}\left(\frac{\mathbf{U}^{\dagger}\boldsymbol{\mathcal{M}}\mathbf{S}_0}{\mathbf{Q}^{\dagger}\boldsymbol{\mathcal{M}}\mathbf{S}_0}\right)=\frac{1}{2}\tan^{-1}\left(\frac{m_{31}+m_{32}}{m_{21}+m_{22}}\right). \tag{15}$$

In the case of a material and scattering direction that does not polarize the light (i.e., when $m_{21}(\theta)\approx 0$, $m_{31}(\theta)\approx 0$), the angle of rotation $\alpha=\gamma'-\gamma$ is the same for any incident polarization and is simply

$$\alpha=\frac{1}{2}\tan^{-1}\left(\frac{m_{32}}{m_{22}}\right). \tag{16}$$

The rotation α in clear media is $[\alpha]_{\lambda}^{T}Cl$, where $[\alpha]_{\lambda}^{T}$ is the specific rotation of glucose at temperature T and wavelength λ, C is the glucose concentration, and l is the interaction length of the photon with the medium. The forward scattering direction, used in the present experiments (i.e., $\theta=0$), simplifies the analysis since $m_{21}(0)$ and $m_{31}(0)$ are near zero,[22] and the interaction length l is approximately the sample length. In addition, by using the forward scattering direction, a comparison of optical rotation in clear and turbid media can be done. Another important experimental polarization parameter is the surviving polarization fraction. The ratio:

$$\beta_L\equiv\frac{m_{22}}{m_{11}} \tag{17}$$

gives the surviving linear polarization fraction, that is, the ratio of the degree of polarizations of the scattered and incident beams when the incident beam is vertically or horizontally polarized.

The object of polarimetry is to experimentally determine one or more elements of the scattering matrix. This is accomplished by measuring the scattered Stokes vector for a known incident Stokes vector to calculate the matrix elements involved in the transformation.[5,23] A difficult task in polarimetry is the measurement of very small elements of the Stokes vector in the presence of large intensity noise in the light beam.

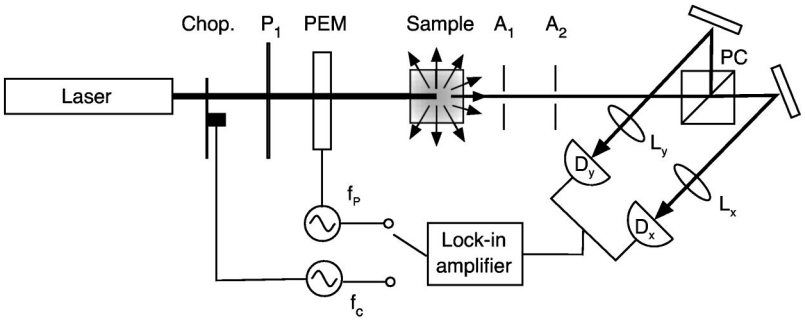

Fig. 2 Schematic diagram of the experimental setup used for the measurements. Chop., mechanical chopper; P_1, polarizer; PEM, photoelastic modulator; A_1, A_2, apertures; PC, polarizing beamsplitter cube; L_x, L_y, lenses; D_x, D_y, photodetectors. f_c and f_p are the modulation frequencies for the mechanical chopper and PEM, respectively.

When the noise is arising from the interaction with a medium, one must resort to statistical averaging of several measurements. However, when the noise originates from the laser beam itself, one can suppress it with an appropriate experimental design. For instance, let the intensity of the laser source be

$$I(t)=I_o+\Delta\tilde{I}(t), \tag{18}$$

where I_o is a constant and $\Delta\tilde{I}(t)$ is the random intensity noise with a time average of zero. Assume a Stokes vector of the form:

$$\mathbf{S}_n(t)=I(t)\begin{bmatrix}1\\ \epsilon\\ 0\\ 0\end{bmatrix}, \tag{19}$$

with $\epsilon \ll 1$, which represents a beam that is noisy [because of the $\Delta\tilde{I}(t)$ term] and only partially horizontally polarized (because of the small value of ϵ). We want to measure the value of ϵ. The measurement can be performed in two steps with a single detector following Eq. (3). The intensity of the horizontally polarized light is measured at time t, then the intensity of the vertically polarized light is measured at a later time t'. Their difference represents an approximation of the value Q of the Stokes vector (which is referred to as $\overline{Q}$), since the measurements are not performed at the same time. The measurement can be represented mathematically by:

$$\overline{Q}=\mathbf{I}^{\dagger}\mathbf{P}(0)\mathbf{S}_n(t)-\mathbf{I}^{\dagger}\mathbf{P}(\pi/2)\mathbf{S}_n(t') \tag{20}$$

$$=\left\{I_o+\frac{\Delta\tilde{I}(t)+\Delta\tilde{I}(t')}{2}\right\}\epsilon+\frac{\Delta\tilde{I}(t)-\Delta\tilde{I}(t')}{2}, \tag{21}$$

where $\mathbf{P}(\theta)$ is the Mueller matrix of a linear polarizer with its axis making an angle θ with the horizontal. The measurement $\overline{Q}$ has the same absolute uncertainty as $I(t)$, which is large if $\epsilon I_o \lesssim [\Delta\tilde{I}(t)-\Delta\tilde{I}(t')]/2$. However, one can use two intensity detectors connected in balanced mode[24] and perform the two measurements simultaneously. Such a detector provides the subtraction of the individual intensity measurements. One obtains the (unnormalized) value of Q directly:

$$\mathbf{I}^{\dagger}\mathbf{P}(0)\mathbf{S}_n(t)-\mathbf{I}^{\dagger}\mathbf{P}(\pi/2)\mathbf{S}_n(t)=\{I_o+\Delta\tilde{I}(t)\}\epsilon\equiv Q, \tag{22}$$

since this measurement reduces to the definition of Eq. (3). The measurement of Q performed with two intensity detectors has the same relative noise as $I(t)$ (i.e., $\Delta\tilde{I}(t)/I_o$) regardless of the value of ϵ because intensity fluctuations cancel upon subtraction. This allows measurements of very small values of the Stokes vector, and therefore precise determination of Mueller matrix elements, even when laser noise is significant (e.g., $\epsilon < \Delta\tilde{I}(t)/I_o$, as is the case with most lasers). We implement this approach experimentally [Eq. (22)] with a balanced detector and use it to determine the small rotation α that is due to the optical activity of glucose in highly turbid solutions using Eq. (16), and determine the surviving polarization fraction using Eq. (17).

3 Materials and Methods

3.1 *Samples*

The turbid samples are suspensions of polystyrene ($n_s=1.59$, density $\rho=1.05$ g/cm^3) spheres in distilled water with a weight fraction $f_w=0.076\%$ (weight of microspheres to weight of water). The spheres have a radius of $r=0.7$ μm, and Mie theory allows the calculation of the scattering efficiency $Q_{\text{ext}}=3.56$ (i.e., the scattering cross-section is $Q_{\text{ext}}\pi r^2$) and anisotropy (the average cosine of the scattering angle) of $g=0.930$ at a wavelength $\lambda=633$ nm.[20] The scattering coefficient $\mu_s=3Q_{\text{ext}}f_w\rho_o/4r\rho$ (with ρ_o the density of water 1 g cm^{-3}) is therefore approximately 30 cm^{-1}, and the reduced scattering coefficient $\mu_s'=(1-g)\mu_s \approx 1.9$ cm^{-1}. The clear and turbid glucose solutions have nominal glucose concentrations ranging typically from 0.001 to 1 M. The actual concentration is determined at the time the solutions are made by measuring the mass of glucose being added to the known water volume.

3.2 *Experimental Setup*

The experimental setup shown schematically in Fig. 2 consists of an unpolarized laser producing approximately 10 mW of power at 633 nm, or about 100 mW at 635 nm. The beam goes through a mechanical chopper, operating at a frequency $f_c=(2\pi)^{-1}\omega_c=200$ Hz, then through a polarizer $P_1(\theta_1)$

oriented with its axis making an angle θ_1 with the horizontal, and a photoelastic modulator (PEM, Hinds, PEM-90) modulating its retardation $\delta(t)$ at frequency $f_p=(2\pi)^{-1}\omega_p$ $=50$ kHz according to a sinusoidal function $\delta(t)$ $=\delta_o \sin \omega_p t$ with its axis horizontal. The amplitude of the retardation modulation δ_o is user specified. The beam then goes through a liquid sample contained in a 1-cm-thick spectroscopic glass cuvette. The light scattered in the forward direction is then apertured with two irises with a 4-mm diameter and separated by 10 cm, and sent to a 2.5-cm-wide polarization splitting cube with a 10^4:1 polarization extinction ratio.

The two beams, linearly polarized along the laboratory vertical and horizontal, are sent to two separate mirrors and focused onto the two photodiodes of a balanced detector (New Focus, Nirvana 2017). The output of the balanced detector is the real-time difference of the measured intensities at both photodiodes, with a 3-dB bandwidth of approximately 100 kHz. A lock-in amplifier (Stanford Research, SR-530), which measures the root mean square (r.m.s.) amplitude of a given harmonic, is used for measuring the 200-Hz signal at the first harmonic of the frequency f_c (while the PEM is turned off) and the 100-kHz signal at the second harmonic of the frequency f_p (while the mechanical chopper is turned off). The combined frequency response function of the photodetector electronics and the lock-in amplifier is identified as $\mathcal{F}(f)$.

3.3 *Methodology*

The angle of the polarizer P_1 is set to $\pi/8$ (22.5 deg). The amplitude- (chopper) and polarization- (PEM) modulated signals are measured independently. The periodic modulation that is due to the mechanical chopper is represented by a periodic square wave $C(t)$ of amplitude 1 and frequency f_c. Using the known Mueller matrix of a polarizer with its axis aligned at θ_1 with respect to the horizontal yields the incident Stokes vector $\mathbf{S}^c$ when only amplitude modulation is present:

$$\mathbf{S}^c = I_o \begin{bmatrix} C(t) \\ \frac{1}{\sqrt{2}} C(t) \\ \frac{1}{\sqrt{2}} C(t) \\ 0 \end{bmatrix}. \tag{23}$$

Upon traversing through the PEM with its modulation axis along the horizontal and with a retardance $\delta(t)$, the phase-modulated Stokes vector $\mathbf{S}^p$ incident on the sample is

$$\mathbf{S}^p = I_o \begin{bmatrix} 1 \\ \frac{1}{\sqrt{2}} \\ \frac{1}{\sqrt{2}} \cos \delta(t) \\ -\frac{1}{\sqrt{2}} \sin \delta(t) \end{bmatrix}. \tag{24}$$

When performing measurements with a lock-in amplifier, a single harmonic of the modulating frequency is measured. A Fourier decomposition of the modulated signal is therefore necessary. The function $C(t)$ representing the mechanical chopper has the following Fourier expansion:

$$C(t) = \frac{1}{2} + \frac{2}{\pi} \sin(\omega_c t) + \frac{2}{3\pi} \sin(3\omega_c t) + \ldots \tag{25}$$

and the sinusoidal phase modulation at the PEM of $\delta(t)$ $=\delta_o \sin \omega_p t$ has the following Fourier expansions:

$$\cos \delta(t) = \cos(\delta_o \sin \omega_p t) = J_0(\delta_o) - 2J_2(\delta_o) \cos 2\omega_p t + \ldots \tag{26}$$

$$\sin \delta(t) = \sin(\delta_o \sin \omega_p t) = 2J_1(\delta_o) \sin \omega_p t + \ldots \tag{27}$$

where $J_n(\delta_o)$ is the Bessel function of the first kind of order n. When performing measurements with the lock-in amplifier at f_c with the mechanical chopper, or at $2f_p$ with the PEM, the multiplicative constants $2\pi^{-1}$ and $2J_2(\delta_o)$ must be included in the analysis. Note that because the balanced detector used in the experiments does not have a uniform frequency response across all modulation frequencies, the frequency response $\mathcal{F}(f)$ must also be considered. The ratio $\mathcal{F}(2f_p)/\mathcal{F}(f_c)$ has been measured to be 0.54 in our setup.

To determine the optical activity of a sample, measurements of Q at frequencies $2f_p$ and f_c are performed and are referred to as Q_{2f_p} and Q_{f_c}, respectively. Using Mueller calculus, Q is obtained for the amplitude-modulated beam in Eq. (23) with $\mathbf{Q}^\dagger \mathcal{M} \mathbf{S}^c$, and for the polarization-modulated beam in Eq. (24) with $\mathbf{Q}^\dagger \mathcal{M} \mathbf{S}^p$. The Fourier expansions, Eq. (25) and Eq. (26), are used to pick the appropriate harmonics and one gets:

$$\frac{Q_{2f_p}}{Q_{f_c}} = \frac{\sqrt{2}\pi \mathcal{F}(2f_p) |J_2(\delta_o) m_{23}|}{\mathcal{F}(f_c) |2m_{21} + \sqrt{2}(m_{22} + m_{23})|}, \tag{28}$$

which can be rearranged to yield:

$$\frac{m_{23}}{\sqrt{2}m_{21} + m_{22}} = \frac{Q_{2f_p}/Q_{f_c}}{\pi J_2(\delta_o) \mathcal{F}(2f_p)/\mathcal{F}(f_c) \pm Q_{2f_p}/Q_{f_c}}. \tag{29}$$

This result is general and does not assume any particular form for the scattering matrix. The sign ambiguity can only be resolved by determining the sign of the optical activity of the solutions (in our case with D-glucose, the sign is positive). It is also known from Monte Carlo simulations[16–18] and symmetry arguments[21] that m_{21} nearly vanishes in the forward-scattered direction in a multiply-scattering material (which comes directly from the fact that m_{21} for a single spherical scatterer vanishes identically in the forward direction[22]). In an optically active medium m_{23} does not vanish and is equal to $-m_{32}$. Therefore from Eq. (29) one gets:

$$\frac{m_{32}}{m_{22}} \simeq -\frac{Q_{2f_p}/Q_{f_c}}{\pi J_2(\delta_o) \mathcal{F}(2f_p)/\mathcal{F}(f_c) \pm Q_{2f_p}/Q_{f_c}}, \tag{30}$$

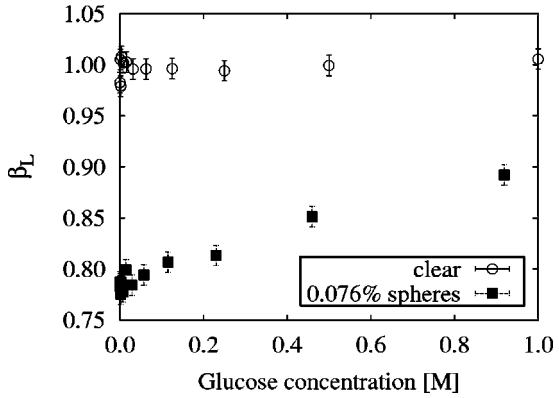

Fig. 3 Surviving linear polarization fraction measured in the forward direction as a function of glucose concentration after propagating through a 1-cm cuvette containing an optically active clear solution (round symbols) and an optically active turbid solution with 0.076% microspheres (square symbols). The latter correspond to scattering coefficients ranging from 28 to 26 cm^{-1}. The error bars, estimated from repeated measurements, are due to the interference of the multiple reflections off the cuvette walls and the slightly different cuvette position at each measurement.

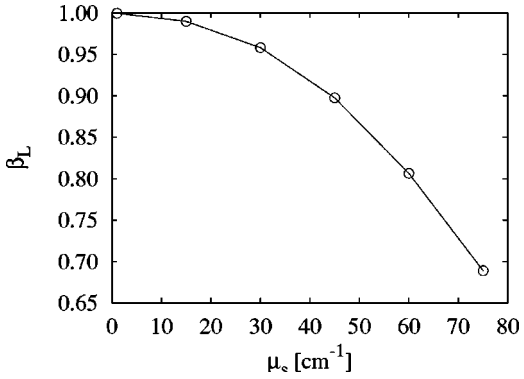

Fig. 4 Calculated surviving linear polarization fraction (β_L) in the forward direction as a function of scattering coefficient from Monte Carlo calculations for a 1-cm cuvette, microspheres of radius 0.7 μm in water, $\lambda = 633$ nm, and no glucose.

which can yield the optical rotation α via Eq. (16). It is also possible to perform the measurements of the intensity I_{f_c} of the scattered beam $\mathbf{S}^c$ in Eq. (23) and obtain:

$$\frac{Q_{f_c}}{I_{f_c}} = \frac{m_{22}}{\sqrt{2}m_{11}} = \frac{\beta_L}{\sqrt{2}}, \tag{31}$$

under the assumption that $m_{22} \gg m_{21}, m_{23}$, and $m_{11} \gg m_{12}, m_{13}$, which is appropriate in high scattering situations. One thus obtains the optical rotation α from Eq. (16) and Eq. (30), and the coefficient of surviving linear polarization fraction β_L from Eq. (31). Although not implemented here, it is noted that if the measurements of the pairs Q_{2f_p} and Q_{f_c}, or Q_{f_c} and I_{f_c} for use in Eqs. (30) or (31) were performed simultaneously, any effects due to multiplicative noise (e.g., slow drift) would be minimized when taking the ratios. Currently, the measurements of the numerator and denominator are independent; therefore the relative uncertainties must be added (hence doubling the uncertainty on the ratio). Simultaneous measurements of both values would lead to a smaller uncertainty on the ratio since the measurements (and their uncertainties) would be correlated.

4 Results and Discussion

From the measurements of Q_{f_c} and I_{f_c}, and with the use of Eq. (31), the surviving linear polarization fraction as a function of glucose concentration is obtained and plotted in Fig. 3, with values ranging from 0.77 to 0.89 for the turbid suspensions ($\mu_s \approx 30$ cm^{-1}). As previously reported,[13] the change in the surviving linear polarization fraction with glucose concentration is due to the increase in the refractive index induced by the dissolved glucose in solution. The index of refraction of water increases by 0.027 per molar of glucose.[10,11] This increase in background index reduces the scattering coefficient μ_s of the suspension[10,11] and therefore increases polarization retention. A Monte Carlo calculation of the surviving linear polarization fraction as a function of scattering coefficient μ_s is shown in Fig. 4. The predicted β_L that matches the measured β_L of Fig. 3 corresponds to a scattering coefficient in the range of 45 to 60 cm^{-1}, which is somewhat higher than, but in general qualitative agreement with the conditions of the experiments (where μ_s is estimated to be approximately 27 cm^{-1}).

Measurements of Q at 2 f_p and f_c are performed and Eqs. (16) and (30) are used to extract the optical rotation of clear and turbid solutions. The results are shown in Fig. 5, along with a linear fit to the data. First, in the case of a clear solution in a 1-cm cuvette and with a laser wavelength of 633 nm, the optical rotation is determined to be 0.82 °M^{-1} cm^{-1}, or a specific rotation of $[\alpha]_{633}^{25°} = (45.5 \pm 0.1)$ deg ml g^{-1} dm^{-1}, at a temperature of 25 °C. This is in agreement with previously estimated values and the expected dependence of the specific rotation on wavelength,[25] and is to our knowledge the first measurement made at that wavelength.

Second, in the case of turbid suspensions, reliable values and linearity of the rotation as a function of glucose concentration are also observed for concentrations around a physiological range as low as 10 mM, which is a notable improvement over our previous results.[12] We note that although the scattering coefficient μ_s and the surviving polarization fraction change slightly with glucose concentration, the linearity of the optical rotation with respect to the glucose concentration is not affected. However, the measured optical rotation is smaller than in the case of a clear solution by approximately 13%, with a slope of 0.72 deg M^{-1} cm^{-1}. This appears to contradict the intuitive argument that in a highly scattering medium photons travel a longer distance than they would in a clear solution before exiting the sample, and therefore they should contribute a larger amount to macroscopic rotation.[12,26] However, a Monte Carlo calculation suggests that this argument is partially right. Although the photons do travel a longer distance, their polarization is also scrambled more and their contribution to the final macroscopic rotation is smaller if μ_s is significant and if the intensity is integrated over a significant area at the exit face.

Figure 6 shows the calculated optical rotation α of a 0.9 M solution of glucose (an optical rotation of 0.74 deg cm^{-1} in a clear medium) using the definition of Eq. (8), as a function of

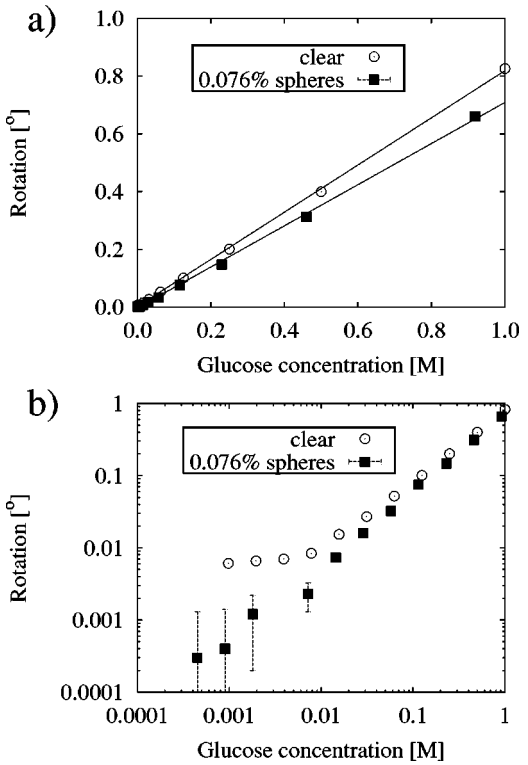

Fig. 5 Linear (a) and logarithmic (b) plots of optical rotation α as a function of D-glucose concentration in a clear (open circles) and turbid (solid square) optically active solution of glucose with 0.076% microspheres. The solid lines are linear fits to the data. For the turbid suspensions, the scattering coefficient ranges from 28 to 26 cm^{-1}. The error bars are smaller than the size of the symbols except for the smallest concentrations.

the β_L for a detected area 5 mm in diameter at the exit face of the cuvette and an acceptance angle of 100 mrad, corresponding to our experiments. It can be seen that when the surviving linear polarization fraction is large $\beta_L > 0.9$ (corresponding to small scattering coefficients), there is indeed an increase in the measured rotation compared with a clear solution. However, for a smaller β_L (and larger scattering coefficients), the measured rotation is smaller. In the conditions of our experiments, where $\beta_L \approx 0.80$ to 0.85, the expected rotation is smaller than in a clear solution by about 10 to 20%, as was measured in our experiments. This is a consequence of the fact that although the average path length of the photons increases with μ_s, their contribution to the rotation decreases faster with μ_s. When all the photons are integrated over an area 5 mm in diameter and with a broad acceptance angle, and Eq. (8) is used, the rotation appears smaller. On the other hand, when a small acceptance angle and a small area are used (i.e., approaching the ideal forward-scattering direction) the range over which the rotation is larger than in clear solutions extends to larger scattering coefficients (Monte Carlo results not shown). We note that although β_L changes slightly with glucose concentration, the change is small enough that the linearity of optical rotation as a function of glucose concentration is not affected enough for the present setup to resolve it. The current limitation on the measurements is the low sensitivity of the silicon photodiodes used in the balanced detector and the low electronic signal obtained.

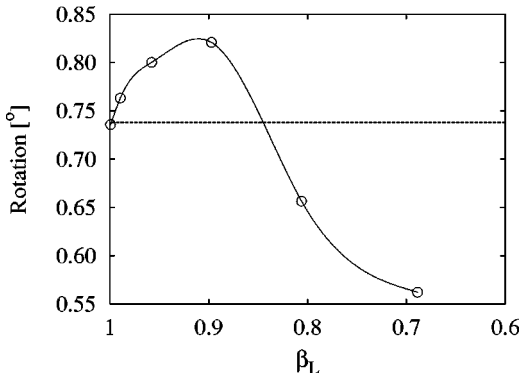

Fig. 6 Monte Carlo calculation of the expected measured rotation as calculated from Eq. (8) in a 1-cm cuvette for a solution with an optical activity of 0.74 deg cm^{-1} as a function of β_L. The solid line is a guide for the eye. The horizontal dashed line is the expected rotation in a clear solution; the Monte Carlo results predict that measurements in a turbid solution of $\beta_L \approx 0.8$ yield a smaller rotation angle by about 15%.

5 Conclusion

We have demonstrated high-precision, low-noise polarimetric measurements in turbid media using balanced detection. The technique allows the rejection of the noise common to the two polarized intensity measurements necessary to determine Stokes parameters, which increases the precision of the measurements. The specific rotation of D-glucose in a clear solution at 633 nm was determined to be $[\alpha]_{633}^{25°} = 45.5$ deg $ml\,g^{-1}\,dm^{-1}$ at room temperature. The surviving linear polarization fractions in chiral (with glucose) and achiral (no glucose) turbid suspensions have been measured in the forward direction and are in reasonable agreement with Monte Carlo calculations. The measurements of optical rotation in turbid suspensions of microspheres demonstrate the possibility of determining glucose concentrations down to levels near 10 mM in a highly scattering and depolarizing medium made of polystyrene spheres. Measurements of optical rotation that is due to glucose in multiply-scattering phantom solutions when the depolarization is significant have been shown to yield slightly smaller values than in clear solutions when intensities are integrated over large areas; this is supported by Monte Carlo calculations.

Acknowledgments

Fruitful discussions with J. Zic and K. Hadley, as well as the financial support of the Natural Sciences and Engineering Research Council of Canada are gratefully acknowledged.

References

1. R. J. McNichols and G. L. Coté, "Optical glucose sensing in biological fluids: an overview," *J. Biomed. Opt.* **5**, 5–16 (2000).
2. J. S. Baba, B. D. Cameron, S. Theru, and G. L. Coté, "Effect of temperature, pH, and corneal birefringence on polarimetric glucose monitoring in the eye," *J. Biomed. Opt.* **7**, 321–328 (2002).
3. A. J. Welch and M. J. van Gemert, Eds., *Optical-Thermal Response of Laser-Irradiated Tissue*, Chap. 2, Plenum, New York (1995).
4. L. H. Wang, S. L. Jacques, and L. Q. Zheng, "MCML-monte Carlo modeling of light transport in multilayered tissue," *Comput. Methods Programs Biomed.* **47**, 131–146 (1995).

5. J. M. Schmitt, A. H. Gandjbakhche, and R. F. Bonner, ''Use of polarized light to discriminate short-path photons in a multiply scattering medium,'' *Appl. Opt.* **31**, 6535–6546 (1992).
6. X. Wang and L. V. Wang, ''Propagation of polarized light in birefringent turbid media: a Monte Carlo study,'' *J. Biomed. Opt.* **7**, 279–290 (2002).
7. J. F. de Boer and T. E. Milner, ''Review of polarization-sensitive optical coherence tomography and Stokes vector determination,'' *J. Biomed. Opt.* **7**, 359–371 (2002).
8. S. Jiao and L. V. Wang, ''Jones-matrix imaging of biological tissues with quadruple-channel optical coherence tomography,'' *J. Biomed. Opt.* **7**, 350–358 (2002).
9. S. L. Jacques, J. C. Ramella-Roman, and K. Lee, ''Imaging skin pathology with polarized light,'' *J. Biomed. Opt.* **7**, 329–340 (2002).
10. M. Kohl, M. Cope, M. Essenpreis, and D. Böcker, ''Influence of glucose concentration on light scattering in tissue-simulating phantoms,'' *Opt. Lett.* **19**, 2170–2172 (1994).
11. J. S. Maier, S. A. Walker, S. Fantini, M. A. Franceschini, and E. Gratton, ''Possible correlation between blood glucose concentration and the reduced scattering coefficient of tissues in the near infrared,'' *Opt. Lett.* **19**, 2062–2064 (1994).
12. I. A. Vitkin and E. Hoskinson, ''Polarization studies in multiply scattering chiral media,'' *Opt. Eng.* **39**, 353–362 (2000).
13. K. C. Hadley and I. A. Vitkin, ''Optical rotation and linear and circular depolarization rates in diffusively scattered light from chiral, racemic, and achiral turbid media,'' *J. Biomed. Opt.* **7**, 291–299 (2002).
14. R. M. A. Azzam, ''Photopolarimetric measurement of the Mueller matrix by Fourier analysis of a single detected signal,'' *Opt. Lett.* **2**, 148–150 (1978).
15. E. Compain and B. Drevillon, ''High-frequency modulation of the four states of polarization of light with a single phase modulator,'' *Rev. Sci. Instrum.* **69**, 1574–1580 (1998).
16. S. Bartel and A. H. Hielscher, ''Monte Carlo simulations of the diffuse backscattering Mueller matrix for highly scattering media,'' *Appl. Opt.* **39**, 1580–1588 (2000).
17. J. R. Mourant, T. M. Johnson, and J. P. Freyer, ''Characterizing mammalian cells and cell phantoms by polarized backscattering fiber-optic measurements,'' *Appl. Opt.* **40**, 5114–5123 (2001).
18. X. Wang, G. Yao, and L. V. Wang, ''Monte Carlo model and single-scattering approximation of the propagation of polarized light in turbid media containing glucose,'' *Appl. Opt.* **41**, 792–801 (2002).
19. C. F. Bohren and D. R. Huffman, *Absorption and Scattering of Light by Small Particles*, Chap. 2, pp. 46–56, Wiley, New York (1983).
20. W. J. Wiscombe, ''Improved Mie scattering algorithms,'' *Appl. Opt.* **19**, 1505–1509 (1980).
21. H. C. van de Hulst, *Light Scattering by Small Particles*, Chap. 5, Dover, New York (1981).
22. C. F. Bohren and D. R. Huffman, *Absorption and Scattering of Light by Small Particles*, Chap. 4, pp. 115, Wiley, New York (1983).
23. E. Collett, ''Measurement of the four Stokes polarization parameters with a single circular polarizer,'' *Opt. Commun.* **52**, 77–80 (1984).
24. P. C. D. Hobbs, ''Reaching the shot noise limit for 10$,'' *Opt. Photonics News* **2**, 17–23 (1991).
25. C. A. Browne and F. W. Zerban, *Physical and Chemical Methods of Sugar Analysis*, Wiley, New York (1941).
26. M. P. Silverman, W. Strange, J. Badoz, and I. A. Vitkin, ''Enhanced optical rotation and diminished depolarization in diffusive scattering from a chiral liquid,'' *Opt. Commun.* **132**, 410–416 (1996).